Bearing Capacity and settlement of ring footings

Gh. Tavakoli Mehrjardi

Technical and Soil Mechanics Laboratory Co., Tehran, Iran
g_tavakoli2000@yahoo.com

ABSTRACT :

Nowadays, more and more ring footings are used in practice. They provide support for structures such as bridge piers, underground stops, water towers, mine, silos and so on. Therefore, the theoretical prediction of ultimate bearing capacity and settlement for ring footings is a requirement in the design. In spite of this fact that a few numerical and experimental studies have been performed to determine the bearing capacity and settlement of these structures for both smooth and rough footings, but there is no collective literature to present the results and design methods to calculate the bearing capacity and settlement of ring footings. In this paper, due to the research which has been done until now, the behavior of ring footing compared with circular footing has been reviewed and the design method of these structures is presented algorithmically

KEYWORDS: Ring footings, Axi-symmetric Structures, Ultimate Bearing Capacity, Settlement, Numerical and Experimental Studies, Circular Footings.

1. INTRODUCTION:

The ring foundations are more suitable and economical to provide support for axi-symmetric structures such as bridge piers, underground stops, water-tower structures, transmission towers, TV antennas (Bowles 1997), silos, chimneys, and storage tanks. For such structures, the ring foundations are preferred because of full utilization of soil capacity and less or no tension condition under the foundation. These foundations generally are subjected to vertical loads due to the superstructure and the horizontal loads due to wind pressure acting on the structure. Depending on the ratio of inside to outside radii, the ring foundations can vary from a relatively narrow circular beam to a circular footing, or a mat with central hole. The latter may be necessary to construct for placing mechanical equipment. With the increasing use of these foundations in many important projects, interest in their behavior has intensified. This behavior includes the load-displacement response and the ultimate bearing capacity.
It is found that there is no collective literature to present the results and design methods to calculate the bearing capacity and settlement of ring footings. In this paper, due to the research which has been done until now, the behavior of ring footing compared with circular footing has been reviewed and the design method of these structures is presented algorithmically.

2. Numerical Study:

Egorov & Nichiporovich (1961) obtained a formulation to calculate the deformation of the bed and the stresses under the ring foundations, is shown in Fig. 1, from the following twin integral equations:

$$\begin{cases} W_0 = \dfrac{2(1-\upsilon^2)}{E}\displaystyle\int_0^\infty D(\alpha)J_0(r\alpha)d\alpha \\ \sigma_0 = \displaystyle\int_0^\infty \alpha D(\alpha)J_0(r\alpha)d\alpha \end{cases} \qquad (2.1)$$

Where w_0 and σ_0 are the deflection and reactive pressures directly under the foundation footing; $J_0(r\alpha)$ is

Bessel's function of the first order and zero sequence; and E and υ are average value of the modulus of deformation and Poisson's ratio of the soil.

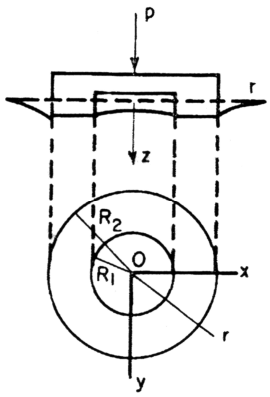

Fig. 1. Axial-symmetrical loading of ring foundation

The obtained formula for the reactive pressures under an absolutely rigid ring foundation is as follows:

$$p(r)=\frac{P}{2\pi R_2 E_0\sqrt{(1-m^2)}}\sqrt{\frac{r^2-m^2R_2^2}{(r^2-R_1^2)(R_2^2-r^2\ )}} \tag{2.2}$$

Where E_0 is a complete elliptical integral of the second order having the form Eq. 2.3.

$$\begin{cases} E_0=\int_0^{\frac{\pi}{2}}\sqrt{(1-K^2\sin^2\theta)}d\theta \\ K^2\ =\dfrac{1-n^2}{1-m^2}, \quad n=\dfrac{R_1}{R_2} \end{cases} \tag{2.3}$$

Calculations show that within the interval $0\le n\le 0.9$ of a ring foundation $m=0.8n$. To determine the settlement of ring footing, the first part of Eq 2.1 can be represented as follows:

$$W_0=\left[P(1-v^2)/ER_2\right]w(n) \tag{2.4}$$

The deflection factor $w(n)$ is given in table 2.1. (Egorov, 1965)

Table 2.1. Values of deflection factor , $\omega(n)$ for assumed values

$N=0$	0.2	0.4	0.6	0.8	0.9	0.95
$w(n)=0.5$	0.5	0.51	0.52	0.57	0.6	0.65

According to Fig. 1 radial displacement at $z=0$ and any point of the boundary of the compressible base, is calculated by Eq. 2.5 and 2.6. (F. N. Borodacheva, 1972)

$$u(r,0)=-\frac{P(1-2\upsilon)(1+\upsilon)}{2\pi ER_2}U(r/R_2) \tag{2.5}$$

$$U(r/R_2)=\frac{R_2}{r}\begin{cases}0 & (0\le r<R_1)\\ 1-\alpha(r) & (n\le r/R_2<1)\\ 1 & (r/R_2>1)\end{cases} \tag{2.6}$$

The numerical values of function $\alpha(r)$ are given in table 2.2.

Table 2.2. Numerical values of $\alpha(r)$

			n=0			
r/R₂	0	0.2	0.4	0.6	0.8	1
$\alpha(r)$	1	0.98	0.917	0.8	0.6	0
			n=0.5			
r/R₂	0.5	0.6	0.7	0.8	0.9	1
$\alpha(r)$	1	0.868	0.762	0.634	0.46	0
			n=0.8			
r/R₂	0.8	0.86	0.9	0.95	1	
$\alpha(r)$	1	0.751	0.597	0.411	0	

Figure 2 shows radial sections of three possible working diagrams (a, b, c) for the region of limiting equilibrium in the bed of a ring foundation, which are distinguished by the inside radius of the ring. (A. M. Karaulov, 2005)

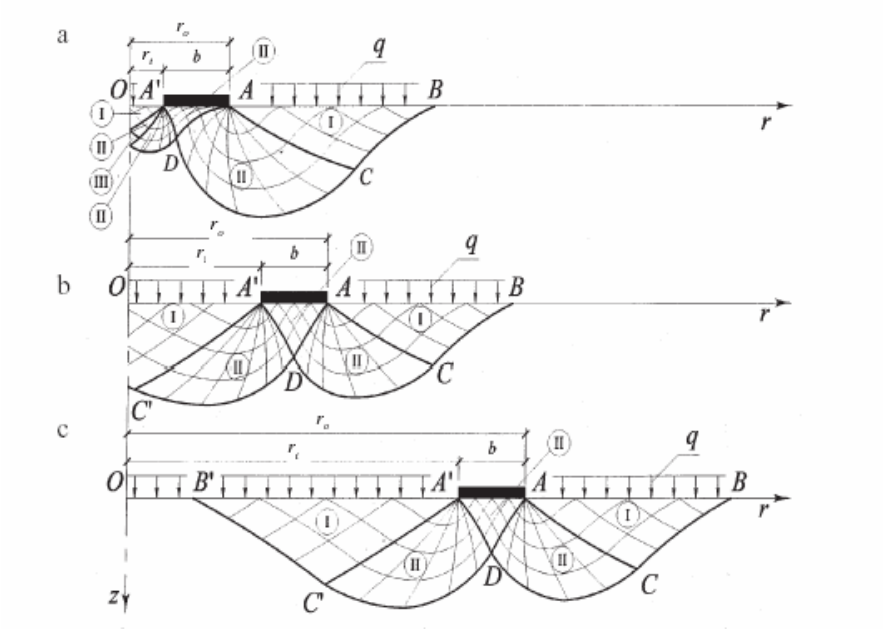

Fig. 2. Working diagrams of region of limiting equilibrium in bed of ring foundation

When $\eta=\frac{r_i}{b}$. is varied from 0 to ∞, the limiting pressure varies from the limiting pressure of a circular foundation to that of a strip foundation on the bed. Therefore it is possible that we define the average pressure (P_{ri}) under a ring footing as follows:

$$P_{ri} = p_s + k(p_c - p_s) \tag{2.7}$$

where p_s and p_c are the average values of the normal component of the limiting pressure on the bed, respectively, of a strip foundation of width b and circular foundation of radius b.
It is obvious that the coefficient k will depend on ϕ, the relative reduced surcharge $q' = (q + C\cot\phi)/\gamma b$, and the ratio $\eta = \frac{r_i}{b}$ (A. M. Karaulov, 2006). Values of the coefficient k were obtained by numerical solution for the indicated range of initial data. The relationship, which approximates the results of the numerical solutions,

$$k = (1 + A\eta)\cos^n \omega; \quad \omega = \frac{\pi}{2}\left(\frac{\eta}{1+\eta}\right)^m \tag{2.8}$$

Which A is defined as Eq. 2.9 that is valid for an infinitely small inside radius.

$$\frac{\partial k}{\partial \eta} = \frac{N_{\gamma c}}{N_{\gamma c} - N_{\gamma s} + q'(N_{qc} - N_{qs})} = A \tag{2.9}$$

Values of m and n are presented in table 2.3 as function of ϕ.

Table 2.3. Values of m and n

ϕ°	M	n
5	0.264	1.363
10	0.365	1.456
15	0.445	1.699
20	0.562	1.899
25	0.696	2.157
30	0.931	2.541
35	1.257	3.048
40	1.766	3.770

Average k values for ϕ of 5 (prior to slash) and 40° (after slash) are given in table 2.4.

Table 2.4. Values of k

η	K values for $\phi = 5^\circ$ and 40° and q of				
	2	4	6	8	10
0	1/1	1/1	1/1	1/1	1/1
0.4	-/1.433	0.363/-	0.406/-	0.397/-	0.404/-
0.8	-/1.095	0.204/1.345	0.214/1.554	0.210/1.562	0.210/1.562
1	-/1.939	0.184/1.196	0.193/1.361	0.191/1.371	0.193/1.376
3	-/0.241	0.096/0.326	0.104/0.384	0.102/0.394	0.105/0.405
5	-/0.142	0.064/0.188	0.071/0.217	0.070/0.221	0.073/0.227

Fig. 3 shows a circular ring footing of inner radius R_1 and outer radius R_2 which is considered on the surface of an elastic stratum of depth h. The footing is assumed to be rigid and rough. The stratum is taken homogeneous. Let F_X, F_Z, M_t and M_r be the amplitudes of the horizontal force, vertical force, torsional

moment and rocking moment on the footing.(Tassoulas J. L. and Kausel E., 1984)

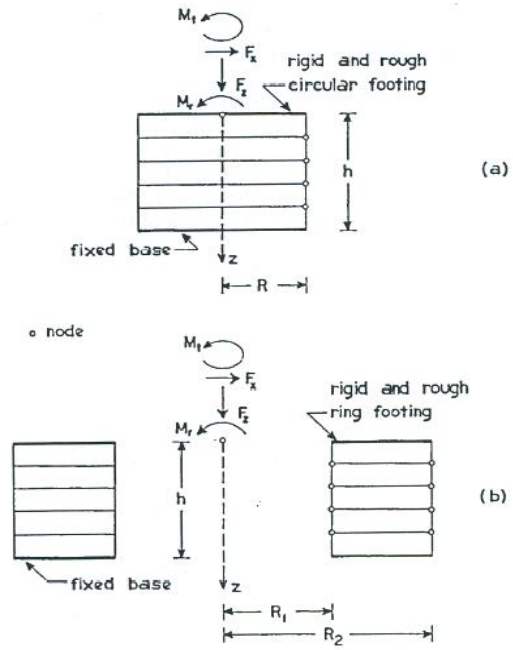

Fig. 3. A ring footing on the surface of a stratum

Let w ،G ،ρ ،ν ،β denote the frequency of time-harmonic vibrations, the shear modulus, mass density, Poisson's ratio and fraction of critical damping in the stratum respectively. The non-dimensional torsional stiffness $\frac{k_{tt}}{GR_2^3}$ is a function of the non-dimensional frequency $\frac{wR_2}{C_T}$ which $C_T = \sqrt{\frac{G}{\rho}}$ is the velocity of transverse waves in the stratum, the depth-to-outer-radius ratio $\frac{h}{R_2}$, the inner-radius -to-outer-radius ratio $\frac{R_1}{R_2}$ and the fraction of critical damping β. It is convenient to use the following normalization:

$$\begin{cases} \dfrac{K_{tt}}{GR_2^3} = \dfrac{K_{tt}^0}{GR_2^3}\left[k_{tt} + i\dfrac{\omega R_2}{C_T}C_{tt}\right](1+2i\beta) \\ \dfrac{K_{zz}}{GR_2} = \dfrac{K_{zz}^0}{GR_2}\left[k_{zz} + i\dfrac{\omega R_2}{C_T}C_{zz}\right](1+2i\beta) \\ \dfrac{K_{xx}}{GR_2} = \dfrac{K_{xx}^0}{GR_2}\left[k_{xx} + i\dfrac{\omega R_2}{C_T}C_{xx}\right](1+2i\beta) \\ \dfrac{K_{rr}}{GR_2^3} = \dfrac{K_{rr}^0}{GR_2^3}\left[k_{rr} + i\dfrac{\omega R_2}{C_T}C_{rr}\right](1+2i\beta) \end{cases} \tag{2.10}$$

$K_{tt}, k_{zz}, k_{xx}, k_{rr}$ are the stiffness coefficients and $C_{tt}, C_{zz}, C_{xx}, C_{rr}$ are the damping coefficients. Finally $\frac{K_{tt}^o}{GR_2^3}, \frac{K_{zz}^o}{GR_2}, \frac{K_{xx}^o}{GR_2}, \frac{K_{rr}^o}{GR_2^3}$ are the non-dimensional static stiffness.

The dynamic stiffnesses were calculated for two different depth $\frac{h}{R_2}=2$ and $\frac{h}{R_2}=3$. Several values of the ratio $\frac{R_1}{R_2}$ were considered. In all cases, $\nu=\frac{1}{3}$ and $\beta=0.05$. Figures 4 and 5 show the non-dimensional stiffnesses as function of the inner-radius -to-outer-radius ratio $\frac{R_1}{R_2}$. The static stiffnesses decrease with increasing $\frac{R_1}{R_2}$. For $\frac{R_1}{R_2}<0.75$ the torsional and rocking static stiffnesses do not deviate significantly from the value corresponding to $R_1=0$. The vertical and horizontal static stiffnesses are somewhat more sensitive to the ratio of the radii of the footing. They deviate considerably from the corresponding static stiffnesses of the circular footing for values of $\frac{R_1}{R_2}>0.6$.

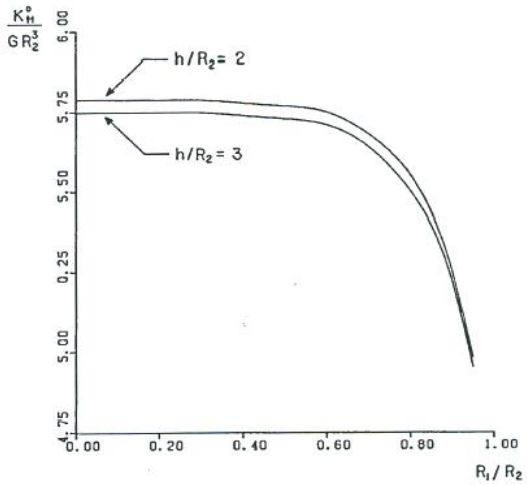

Fig. 4. Static torsional stiffness

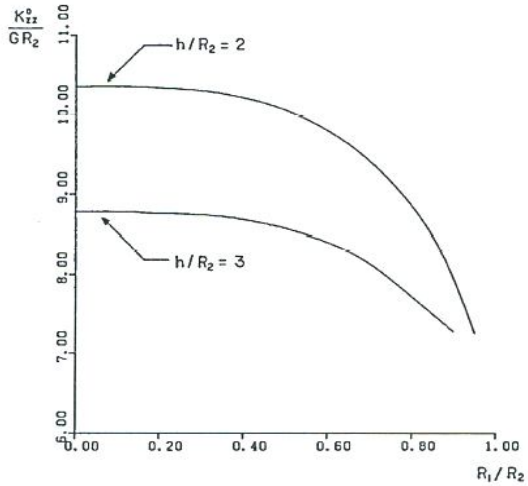

Fig 5. Static vertical stiffness

The stiffness and damping coefficients for $\frac{h}{R_2}=2$ are plotted vs. the non-dimensional frequency $\frac{1}{2\pi}(\frac{WR_2}{C_T})$ for $\frac{R_1}{R_2}=0,0.5,0.8,0.9$ in figures 6. There is little change in the coefficients for the different values of the ratio $\frac{R_1}{R_2}$, especially in the lower frequency range, $0\le\frac{1}{2\pi}(\frac{WR_2}{C_T})\le 0.25$. There is a shift in the peaks and troughs of the curves as $\frac{R_1}{R_2}$ increases: the characteristic frequencies at which maxima and minima occur are lower for higher values of this ratio, or equivalently for lower static stiffness of the ring footing. It must also be noted that the difference between the coefficients for $\frac{R_1}{R_2}=0$ and $\frac{R_1}{R_2}=0.5$ is relatively very small.

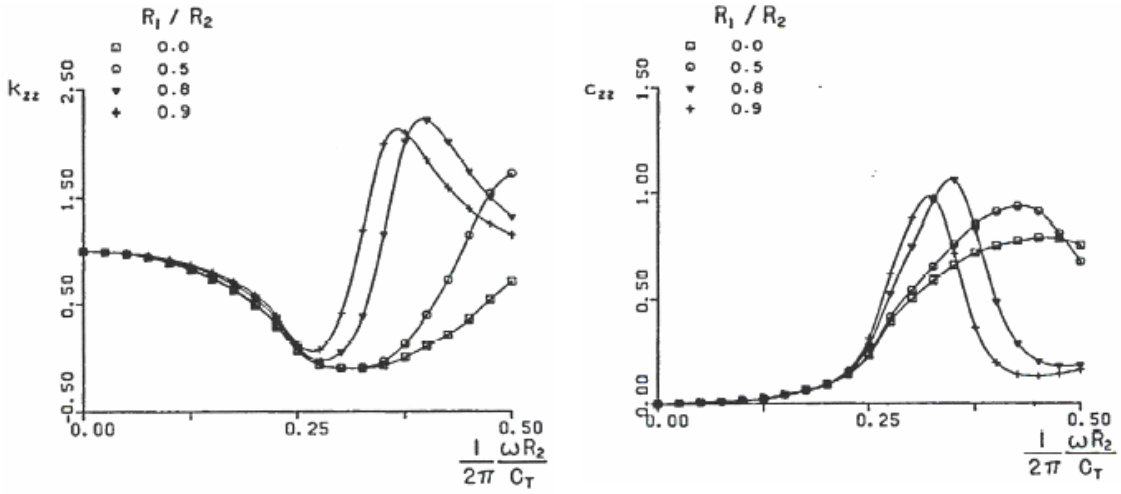

Fig. 6. Vertical stiffness and damping coefficients

3. Experimental Study:

In order to study the behavior of ring footing under vertical and lateral loads, S.Saran and et. al (1987) had done some tests on sand. Tests had been carried out on 20 cm external diameter and the ratio of $n = \frac{b}{B} = 0,\ 0.2,\ 0.4,\ 0.6,\ 0.8$. The Fig. 7 illustrates that as the value of n increases, the ultimate capacity also increases and attains a peak value at $n = 0.4$. As the value of n increases further, there is decrease in ultimate capacity owing to the phenomenon of aching of soil at the annuli. Hataf and Boushehrian (2003) studied on the effect of changing n on BCR of ring footing for unreinforced soil which is shown in Fig. 8. As it can be found, the maximum BCR has occurred at $n = 0.4$.

Fig. 9 shows the plot of variation of settlement with n at constant pressure of $0.4\frac{kg}{cm^2}$. It is evident from this figure that settlement of the footing decrease of n. This decrease in settlement may be due to the fact that the increase in the size of annuli the width of ring $\frac{(B-b)}{2}$ decreases.

Fischer (1957) presented a solution for the settlement of a flexible ring plate on an elastic isotropic half-space. The solutions are given in Eq. 3.1 where S_e and S_i are settlement of the outside and inside edge points, respectively, of the ring plate; S_m is average settlement; S_o is settlement of the center of a full circular flexible plate and I_e, I_i, I_m are influence factors that are functions of the ratio inside radii (r_i) to outside radii (r_o).

$$\begin{aligned} S_e &= S_o I_e \\ S_i &= S_o I_i \\ S_m &= S_o I_m \end{aligned} \tag{3.1}$$

$$S_o = \frac{qD(1-v^2)}{E} \tag{3.2}$$

The influence factors I_e, I_i, I_m are given in Fig. 10.

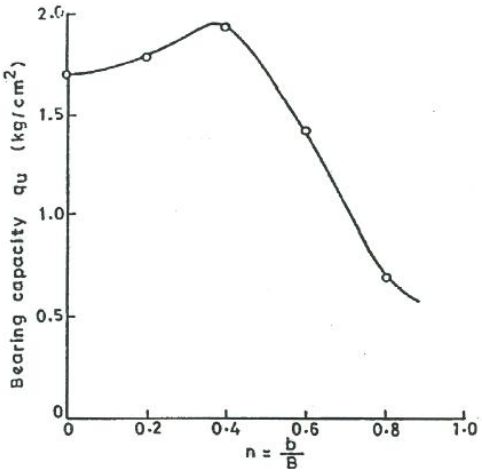

Fig. 7. Effect of n

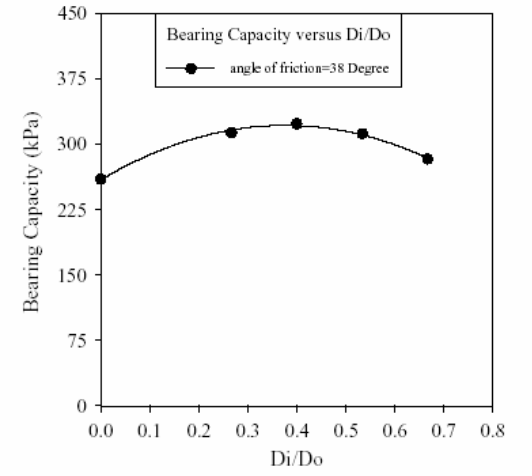

Fig. 18. Effect of $n = \frac{D_i}{D_o}$

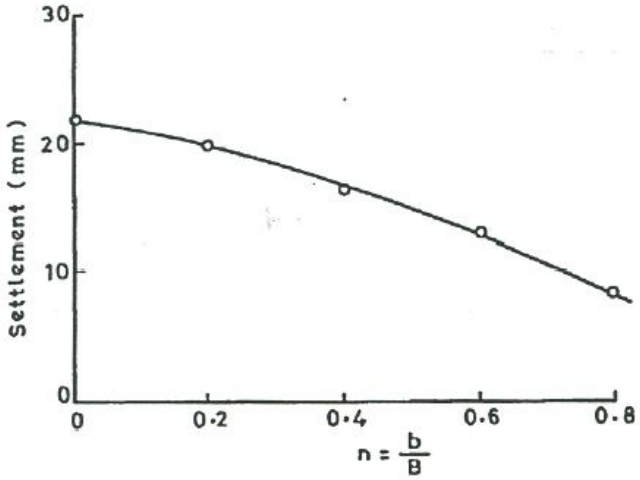

Fig. 9. Variation of settlement with n at constant pressure

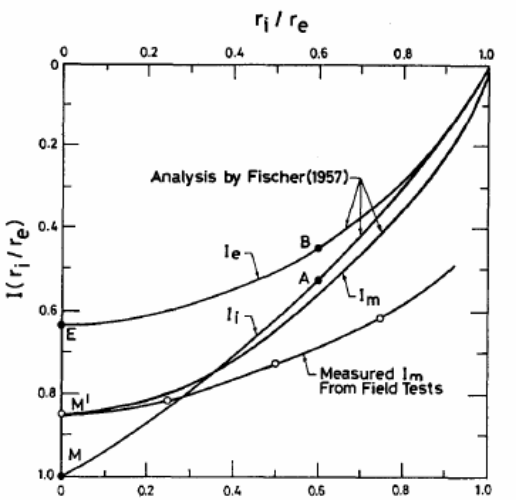

Fig. 10. Influence factors for settlement

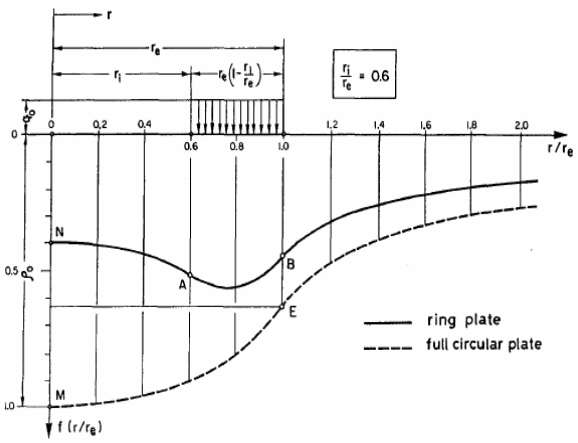

Fig. 11. Variation of influence factor

Fig. 11 shows the influence factors, as presented by Fischer, for the settlement of the ring plate within a distance r of two outside radii from the center for the case of $\frac{r_i}{r_o} = 0.6$. The points A and B correspond to those in Fig. 10. Also shown in Fig. 11 are the settlement influence factors for a full circular flexible plate. Points E and M present settlement of the edge and center, respectively.

Variation of lateral load capacity P_u with n for $\frac{h}{B} = 0.3$ (h is the height of applied horizontal load) is shown in Fig. 12. These plots indicate that value of P_u decreases with the increase in n owing to decrease in contact surface and friction force.

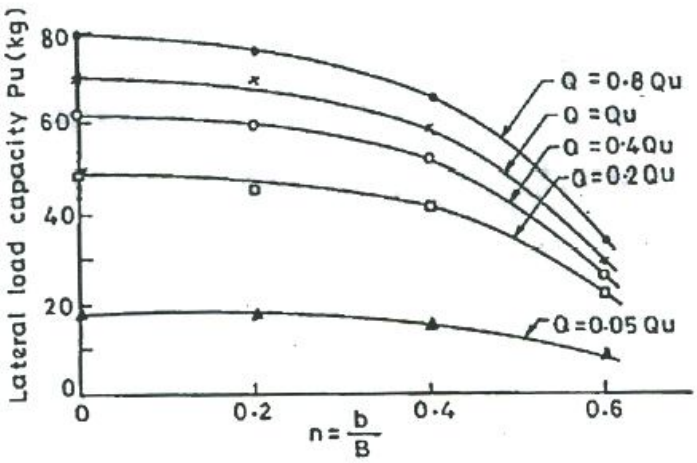

Fig. 12. Effect of n on lateral load capacity

In Fig. 13 the effect of increasing N on BCR is evident, (Hataf and Boushehrian, 2003). However, for $N > 4$ this effect is negligible. This is because the depth of influence under the footing in both cases (i.e. circular and ring footing) affected by loading (i.e. extent of stress bulb) is finite beyond which replacing reinforcement has not any effect on bearing capacity improvement. In some of the results reported (Guido et al., 1985; Yetimuglu et al., 1994; Adams and Colin, 1997) even a decrease in BCR after a certain number of layers has been observed which might be related to the lateral inter-slip of soil and reinforcement layers.

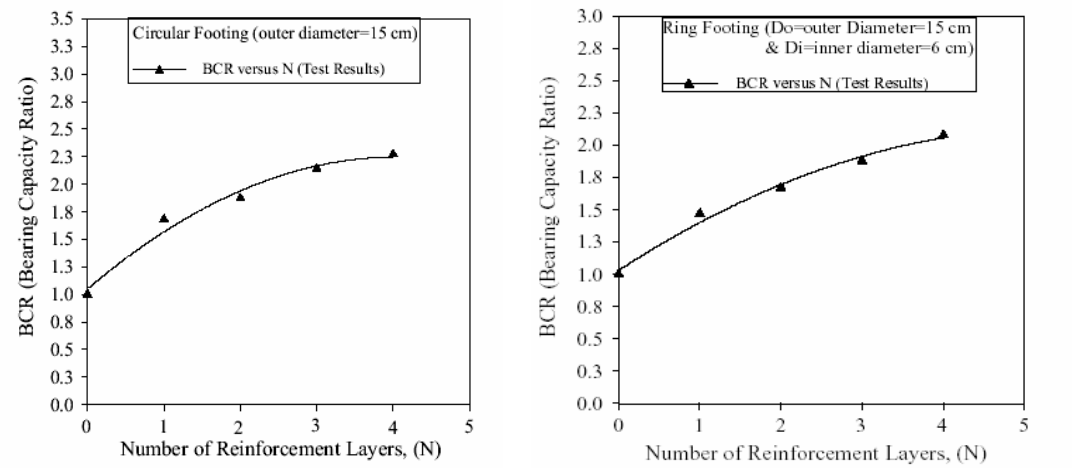

Fig. 13. BCR variation with N for ring and circular footings

Due to the low value of relative density for the sand, the failure mode was found to be punching failure.

3. Conclusion

The ring foundations are more suitable and economical to provide support for axi-symmetric structures such as bridge piers, underground stops, water-tower structures, transmission towers, TV antennas, silos, and chimney. In order to reach the maximum bearing capacity from the ring footing, the ratio of inner radius to outer radius should be selected equal to 0.4. The settlement of the footing decrease with n. This decrease in settlement may be due to the fact that the increase in the size of annuli the width of ring decreases. Depending on n, the behavior of this system defer from full circular footing to strip footing and the failure of it vary from general shear failure to the punching failure respectively.
In order to calculate the bearing capacity of ring footings, it recommends to follow as below:

1) Calculate the bearing capacity of string footing q_s with the width of ring footing $b = r_o - r_i$ due to the soil characteristic.
2) Calculate the bearing capacity of circular footing q_c which the diameter of that is $b = 2(r_o - r_i)$ due to the soil characteristic.
3) Calculate the k factor due to table 2.4 and values of ϕ, η, q. It should be noted that use the interpolation to obtain k factor for the other values of ϕ which is not mentioned in table 2.4.
4) According to Eq. 2.7, it is possible to obtain bearing capacity of the ring footings.

Acknowledgements:

The financial support from Technical and Soil Mechanics Laboratory Co. (Project No. RSI-86S1RSP01 2007) is gratefully acknowledged. The author is also thankful for the help provide by Mr. Barzegar, the head of TSML, Mr. Ismaeli, Mr. Nazar Nejad, Mr. Taheri and Mr. Jamshidi.

References:

FISCHER, K. (1957). "Zur Berechnung der Setzung von Foundamenten in der form einer Kreisforgisen ring flache". Der Bauingeniour. **N 32**.

Bowles JE. Foundation analysis and design. New York: McGraw-Hill; 1997.

Egorov, K.E, and A.A. Nichiporovich (1961). Research on the Deflection of foundations. Proc. Fifth International Conference on Soil Mechanics and Foundation Engineering, **Vol.1**, PP. 861-6.

Egorov, K.E. (1965). Calculation of Bed for Foundation with Ring Footing.

Borodacheva F. N. (1972). Displacements and Stresses in the Base of a Rigid, Symmetrically Loaded Ring Foundation. *Fundamenty I Mekhanika Gruntov*, **No. 4**, PP. 1-3.

Karaulov A. M. (2005). Static Solution of the Limiting-Pressure Problem for Ring Foundations on Soil Beds. *Fundamenty I Mekhanika Gruntov*, **No. 6**, PP. 2-5.

Karaulov A. M. (2006). Experimental and Theoretical Researchon the Bearing Capacity of Ring Foundations Beds. *Fundamenty I Mekhanika Gruntov*, **No. 2**, PP. 2-4.

Tassoulas J. L. and Kausel E. (1984). On the Dynamic Stiffness of Circular Ring Footings On an Elastic Stratum. *International Journal For Numerical and Analytical Methods in Geomechanics*. **Vol: 8**, 411-426.

S.Saran and et. Al. (1987). Behavior of Ring Footings on Sand Under Vertical and Horizontal Loads. 9Th Southeast Asian Geotechnical Conference Bangkok-Thailand. Section: 6, 79-88.

Boushehrian J.H. and Hataf N. (2003). Experimental and numerical investigation of the bearing capacity of model circular and ring footings on reinforced sand. *Geotextiles and Geomembranes*; **Vol: 21**, 241-56.

Guido V.A., Biesiadecki, G.L. and Sullivan and M.J. (1985). Bearing Capacity of Geotextile Reinforced Foundation. Proceedings of the 11th International Conference on Soil Mechanics and Foundation of Engineers, San Francisco, CA, 1777-1780.

Yetimuglu T., Wu J.T.H. and Saglamar A. (1994). Bearing capacity of rectangular footing on geogrid-reinforced sand. *Journal of Geotechnical Engineering ASCE* **120(12)**, 2083-2099.

Adams M.T and Colin J.G. (1997). Large model spread footing load tests on geosynthetic reinforced soil foundation. *Journal of Geotechnical Engineering ASCE* **123 (1)**, 66-73.